Catal Lett (2009) 127:158–166
DOI 10.1007/s10562-008-9662-7

Properties and Activity of Al_2O_3 + ZSM-5 Supported Ni and NiRu Catalysts in 1-Methylnaphthalene Hydrogenation: Effect of Ni Incorporation Method and Calcining Procedure

Aleksandra Masalska

Received: 7 July 2008 / Accepted: 10 September 2008 / Published online: 7 October 2008

Abstract Ni (8 wt.% NiO) and NiRu (8 wt.% NiO and 1.1 wt.% RuO_2) dewaxing catalysts containing a ZSM-5 zeolite were examined in the hydroconversion of 1-methylnaphthalene. The effect of the Ni incorporation method and thermal treatment of the Ni catalyst was examined. The catalysts were characterized by XRF, N_2-sorption, TPR, H_2-chemisorption, XPS, XRD and TPD-NH_3. It has been found that the use of calcination in air for the decomposition of nickel nitrate deteriorates the activity of the Ni catalyst to the greatest extent. Ru not only enhances catalyst activity but also reduces the differences in activity resulting from the various methods of Ni catalyst preparation.

Keywords Ni catalyst · RuNi catalysts · 1-MN hydrogenation

1 Introduction

The continuingly increasing demand for diesel fuel is covered, inter alia, by adding components from destruction processes. Such a procedure accounts for the increase in the content of aromatics (e.g., LCO from FCC contains up to 80 vol.% of aromatics [1]) and for the deterioration of the cold flow properties (e.g., diesel oil fraction from hydrocracking [2]). In a recent study [3] we have observed that over Ni-based dewaxing catalysts with a Ru-modified hydrogenation function the conversion of *n*-paraffin occurred simultaneously with the hydrogenation of aromatic hydrocarbons. Ru has been chosen as a second metal not only owing to a high hydrogenating activity (low heat of H_2 adsorption [4]) but also because of a high thiotolerance as compared to other monometallic noble metal catalysts [5, 6]. Our studies have revealed that Ru increases both the reducibility of Ni oxide species and Ni dispersion. A similar promoting action of the second metal has been reported elsewhere [7, 8]. Some researches suggest that the second metal as a promoter affects catalytic performance by preventing the formation of carbonaceous deposits [9, 10] or inducing a cluster or ligand effect [11]. We have found that the activity of NiRu/ZSM-5 + Al_2O_3 catalysts depended both on the Ru content and on the method of Ni catalyst preparation [3]. The catalysts examined differred not only in the method of combining alumina and zeolite but also in the procedure of Ni incorporation. For the decomposition of metal precursors, use was made of calcination in air. During calcination in air a strong interaction occurs between Ni oxide species and alumina, which leads to the formation of Ni–Al oxide spinels on the catalyst surface. Such interactions have been reported by many authors [12–14]. Although nickel aluminates exert a stabilising effect on nickel particles [15], their occurrence is not desired for two reasons: they are catalytically inactive and limit the effective utilisation of the incorporated metal.

The literature also includes references to the preparation of Ru calatysts suggesting that the stage of calcination should be avoided to prevent the agglomeration of Ru particles in the presence of O_2 (which occurs at a relatively low temperature, i.e., at about 150 °C) [16]. Eliche-Quesada et al. [6] have revealed that a Ru catalyst (5 wt.%) on mesoporous silica, which was calcined (400 °C, 2 h) prior

---

The work was presented during the conference "Catalysis for Society", Krakow, May 11-15, 2008.

A. Masalska (✉)
Faculty of Chemistry, Wrocław University of Technology,
7/9 Gdańska Street, 50-344 Wrocław, Poland
e-mail: aleksandra.masalska@pwr.wroc.pl

to reduction, displays a lower dispersion of Ru (by 30%) than when reduction was performed without calcination as a prior step. The calcination increased the average diameter of the metallic crystallites from 2.4 to 13.5 nm. Mazzieri et al. [17] have observed the same calcination effect. In their study, the dispersion of Ru on Al_2O_3 (4% Ru), which was made subject to calcination (500 °C, 3 h) followed by reduction, amounted to 5%, whereas that of the same catalyst subjected to reduction alone equalled 19%.

These findings have prompted us to address the problem of how the method of Ni incorporation and the thermal treatment of Ni catalysts influence the physicochemical properties and the hydrogenating activity of Ni and NiRu dewaxing catalysts. The hydrogenating function of the catalysts is expressed in terms of their activity in 1-methylnaphthalene (1-MN) hydrogenation.

2 Experimental

2.1 Catalysts Preparation

Studied were Ni and NiRu (8 wt.% NiO; 1.1 wt.% RuO_2) catalysts on Al_2O_3 + ZSM-5 (1:1) supports, the precursors of metals being $Ni(NO_3)_2\ 6H_2O$ and Ru(III) acetylacetonate. Catalyst code and preparation procedure are compiled in Table 1.

In the preparation of Ni catalysts, nickel was incorporated by impregnation in a one-step procedure at the pH of 1.8 and 4.8 (catalyst code Ni-1 and Ni-2, respectively). For the decomposition of $Ni(NO_3)_2$ the catalysts were treated under H_2 flow. In the case of the catalysts referred to as Ni-3 and Ni-4, nickel was incorporated in a two-step procedure (F + I): half the metal at the stage of support formation (F) and the other half at the stage of impregnation (I) at pH = 4.8. After stage (F), Ni-3 and Ni-4 catalysts were calcined in air for the decomposition of $Ni(NO_3)_2$. After stage (I), the Ni-3 catalyst was treated under H_2 flow and the Ni-4 catalyst was calcined in air. Treatment under H_2 flow (50 mL/min) was conducted at 2°/min to 300 °C and thereafter at 5°/min to 500 °C (for 3 h). Calcination in air was performed in a furnace at 200 °C (1 h), 300 °C (1 h) and 400 °C (2 h).

RuNi catalysts were prepared by impregnation of Ni catalysts (dried or calcined) with an alcohol solution of Ru(III) acetylacetonate. After drying at 50 °C in a vacuum drier, all RuNi samples were treated in H_2 flow for the decomposition of the Ru precursor in the regime described above. The samples were then cooled down to room temperature also in the stream of H_2. Thus, RuNi-1 and RuNi-2 were obtained by impregnation with Ru precursor of dried nickel catalysts ($Ni(NO_3)_2/Al_2O_3$ + ZSM-5). The

Table 1 Catalyst code and preparation procedure

Method of Ni catalyst preparation			
Ni-1	One-step procedure (I):	Impregnation at pH = 1.8	Followed by treatment in H_2 flow at 500 °C.
Ni-2		Impregnation at pH = 4.8	
Ni-3	Two-step procedure (F + I): half the Ni incorporated at the stage of support formation (F) followed by calcination in air at 500 °C; the other half at the stage of impregnation (I) at pH = 4.8		Followed by treatment in H_2 flow at 500 °C.
Ni-4			Followed by calcination in air at 500 °C.
Method of RuNi catalyst preparation			
RuNi-1	Ni incorporated during one-step impregnation at pH = 1.8 followed by drying at 120°C.		Impregnation of nickel catalysts with Ru precursor followed by treatment in H_2 flow at 500°C.
RuNi-2	Ni incorporated during one-step impregnation at pH = 4.8 followed by drying at 120°C.		
RuNi-3	Ni catalyst obtained in two-step procedure (F + I); calcined in air after stage F and dried after stage I.		
RuNi-4	Ni catalyst obtained in two-step procedure (F + I); calcined twice: after stage F and stage I.		

RuNi-3 catalyst was prepared by impregnating the $Ni(NO_3)_2/NiO/Al_2O_3$ + ZSM-5 catalyst; Ni catalyst was calcined in air after stage (F) and dried after stage (I). In the preparation of the catalyst referred to as RuNi-4, ruthenium was incorporated by impregnation of the twofold calcined nickel catalyst, after stage F and stage I (NiO/Al_2O_3 + ZSM-5).

2.2 Catalyst Characterisation

2.2.1 *Porous Structure and Acidity*

Prior to measurements, the sample was outgased under vacuum conditions at 150 °C for 1 h. N_2 adsorption was measured at 77 K with a Quantachrome Autosorb Automated Gas Sorption System. Acidity was determined via chemisorption of ammonia at 180 °C in a through-flow system using a katharometer as a detector. More details can be found in a previous paper [18].

2.2.2 *Chemical Analysis and H_2 Chemisorption*

Ni and Ru content was established using a X-ray fluorescence technique. The H_2 volume adsorbed was measured at using Micromeritics ASAP 2010C. The samples were reduced in a H_2 stream at 500 °C (1 h). The Ni–Ru system was characterised only in terms of the volume of the H_2 adsorbed because in this bimetallic system adsorption temperature differs from one metal to another.

2.2.3 *TPR Experiments*

Use was made of an Altamira AMI-1 system. The TPR of the catalyst was conducted up to 850 °C, using a mixture which contained 80 vol. % of Ar and 20 vol. % of H_2 (>99.999%); gas velocity and heating rate were 40 cm^3/min and 15°/min, respectively. Before TPR run all samples were oxidized in an argon stream containing 15% O_2 at 500 °C for 30 min.

2.2.4 *XRD Examinations*

XRD patterns were obtained using a PANalytical X'Pert ProMPD diffractometer with a PW3050/65 high resolution goniometer, at 40 kV and 30 mA (Cu$K\alpha$). Data were collected over the 2θ range of 5 to 90° with a step size of 0.0167 and a 25.8-s time per step. The diffractograms were compared with the one taken from the JCPDX index.

2.2.5 *X-ray Photoelectron Spectroscopy*

XPS measurements were performed using a SPECS PHOIBOS 100 spectrometer with Mg$K\alpha$ radiation. The spectrometer was calibrated with the Au $4f_{7/2}$, Ag $3d_{5/2}$ and Cu $2p_{3/2}$ lines at 84.2, 367.9 and 932.4 eV, respectively. The Al 2p line (at 73.83 eV) was used as a reference. A nonlinear least-square fitting algorithm was applied using peaks with a mix of Gaussian and Lorentzian shape and a Shirley baseline.

2.2.6 *Catalytic Experiments*

Catalytic activity was tested using 1-methylnaphthalene (1-MN) at atmospheric pressure in a fixed-bed reactor. The catalyst (100 mg) was activated in H_2 flow up to 500 °C (1 h) at a heating rate of 5°/min. Experiments were conducted at 200–260 °C and a contact time of 0.15–0.5 s. The reaction products were analysed on line by gas chromatography (FID, RTX-1). The measure of the catalyst's stability was the conversion at 200 °C before and after the activity test cycle, which included the influence of reaction temperature or the influence of both temperature and contact time.

3 Results and Discussion

3.1 Ni Catalysts

The chemical composition of the catalysts shows that the content of Ni is close to the nominal one (8 wt.% NiO) independently of the preparation method applied. All Ni catalysts display a similar surface area and total pore volume (Table 2). The catalysts differ, however, in the BHJ pore diameter (which varies from 3.8 to 6.5 nm) and micropore volume (which is lower for Ni-3 and Ni-4 than Ni-1 and Ni-2). H_2-chemisorption measurements have revealed that Ni-1 and Ni-2 display a noticeably higher dispersion than do Ni-3 and Ni-4. The Ni-4 catalyst displays the lowest dispersion, which is one-fourth that of Ni-1 and Ni-2, and less than one half that of Ni-3.

None of the catalysts tested shows characteristic X-ray diffraction lines for Ni, NiO and $NiAl_2O_4$ (results not shown), which can be attributed to the high dispersion or to the poor crystallinity of these species. Only a splitting of the strongest line at 23.10 2θ, which is characteristic for the Ni-form of the ZSM-5 zeolite, was observed in the diffractograms.

The NH_3-TPD results indicate that the acidity of Ni-4 (whose preparation involved twofold calcination) is the lowest, primarily owing to the decrease in the acidity of the centres which desorb ammonia at 300–450 °C. The highest acidity was that of Ni-2, whose preparation included one-step impregnation with nickel nitrate at pH = 4.8. During impregnation at pH = 4.8 nickel occurs in the form of large tetrameric nickel ions acting as Lewis acid sites and is deposited mainly on the external surface of the support.

Table 2 Physicochemical properties of the catalysts

Catalyst Code	Metal content[a] (wt.%)		D (%)	V^b (cm^3/g)	S_{MET} (m^2/g_{sample})	Reducibility[c] (a.u.)	Surface area (m^2/g)		Pore volume (cm^3/g)		BJH pore diameter (nm)	Acidity (mmol NH_3/g)
	NiO	RuO_2					S_{BET}	St^d	$V_{total}{}^e$	$V^d{}_{MIK}$		
Ni-1	7.9	–	16	1.90	6.6	923	295	147	0.32	0.064	3.8	0.96
Ni-2	8.1	–	18	2.12	7.4	1,045	281	134	0.32	0.061	6.5	0.99
Ni-3	8.2	–	10	1.21	4.2	787	280	160	0.33	0.052	4.9	0.96
Ni-4	8.1	–	4	0.45	1.55	613	278	160	0.33	0.051	5.6	0.94
RuNi-1	7.8	1.09	–	3.21	–	1,062	281	158	0.33	0.053	4.3	0.92
RuNi-2	8.0	1.04	–	3.56	–	1,243	251	123	0.28	0.053	6.5	0.94
RuNi-3	8.1	1.08	–	2.79	–	1,005	250	138	0.31	0.048	4.9	0.91
RuNi-4	8.0	1.09	–	1.72	–	886	253	157	0.32	0.041	5.6	0.89

[a] As determined by XRF

[b] Volume of hydrogen adsorbed

[c] Hydrogen uptake up to 500 °C (TPR)

[d] Calculated from t-plot

[e] Calculated at relative pressure $p/p_0 = 0.99$

TPR experiments were used to investigate the interaction between nickel and support (ZSM-5 + Al_2O_3). Compared to alumina, the interaction of NiO with the zeolite is rather poor. There is a probability, however, that after high temperature steaming or acid treatment of the zeolite, the interaction between nickel and the external surface of the zeolite will be stronger [19] and that the reaction of Ni^{2+} with the extra framework aluminium species will result in the formation of the Ni–Al spinels [20]. In our study, the Ni-support interaction will be considered as the Ni-alumina interaction. The TPR patterns (Fig. 1) have revealed that the method of Ni incorporation and the conditions of thermal treatment for the decomposition of nickel nitrate influence the reducibility of the Ni species. For all the catalysts examined, the reduction of the NiO species initiates at temperatures varying between 240 and 260 °C. The reducibility of the catalysts whose preparation involved one-step impregnation and treatment in H_2 flow was found to be the highest. The TPR profiles for these catalysts display one main peak of reduction with a maximum at 400 °C. There are references in the literature [12, 21] demonstrating that below 500 °C the amorphous overlayer of NiO whose interaction with the support is poor undergoes reduction. The slight shift of the reduction peak towards higher temperatures, as well as the broadening of the peak for Ni-1, indicates that the interaction of the Ni species with the support is stronger with Ni-1 than Ni-2. The profile of Ni-3, the one whose preparation involved a two-stage Ni incorporation (F + I), calcination in air after stage (F) and thermal treatment in H_2 flow after stage (I), is characterised by two main regions of reduction: 300–500 °C and 700–850 °C. The latter temperature range is ascribed to the reduction of the Ni–Al oxides spinels resulting from the strong interactions between Ni oxide species and alumina. The TPR pattern for Ni-4, whose preparation included twofold calcination in air (after stages F and I), displays an additional, distinct reduction region at 500–700 °C with a broad maximum at 520–600 °C. This is the range of reduction for the amorphous overlayer of NiO, which is not chemically bound but interacts with the support stronger than does the amorphous overlayer of NiO, which reduces below 500 °C [21]. It is essential to note that, compared to Ni-3, Ni-4 shows a decrease in the proportion of NiO, whose interaction with the support is poorer, and an increase in the proportion of Ni–Al oxide spinels. As can be seen from the TPR run, in the case of Ni-4, the amount of the Ni atoms that failed to undergo reduction at 850 °C is higher than in the case of the other Ni catalysts.

X-ray photoelectron spectroscopy was used to examine the surface composition and the chemical state of Ni catalysts. Table 3 compiles the atomic chemical composition and the Ni/Al + Si atomic ratios, as well as the BE data for the Ni species obtained upon deconvolution of the Ni $2p_{3/2}$ region. The XPS spectra have revealed peaks at BE 853.1 and 855.6 eV corresponding closely to the values reported for metallic Ni (853.0 eV [15]) and NiO (854.0–855.0 eV [15, 22]). The presence of metallic Ni and stoichiometric NiO at BE showing values slightly higher than 853.0 and 855.0 eV (characteristic for pure Ni and NiO) suggests the occurrence of weak interactions with the support. According to literature [15, 20, 22, 23], the signals at higher BE (856.5–857.2 eV) can be assigned to Ni aluminate species.

The results of XPS clearly show that the differences in the preparation procedure influenced the relative concentrations of nickel atoms on the catalyst surface. As can be seen from the data in Table 3, the Ni/Al + Si ratio for Ni-1

Fig. 1 TPR patterns for Ni and RuNi catalysts (after treatment at 500 °C for 30 min in a mixture containing 15% O_2 in He)

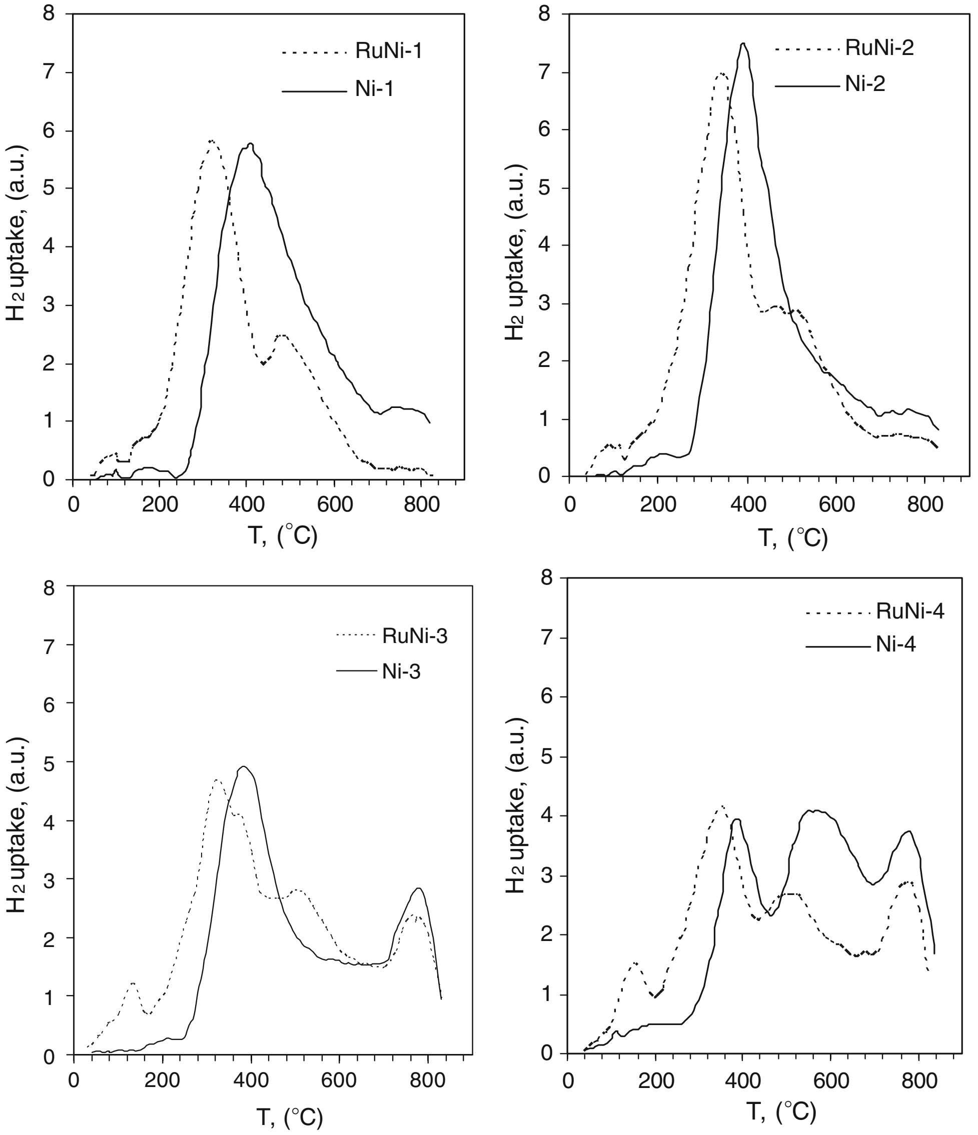

Table 3 XPS characterisation of catalysts (after reduction at 500 °C forl h)

Catalyst	Surface atomic chemical composition (%)					Atomic ratio		BE (eV) of Ni $2p_{3/2}$ levels after deconvolution		
	O	Al	Si	Ni	Ru	Ni/Ru	Ni/Al + Si	Nio (853.1 eV)	NiO (855.6 eV)	$NiAlO_4$ (857.2 eV)
Ni-1	64.7	25.5	8.0	1.85	–	–	0.055	31*	57*	12*
Ni-2	65.6	25.5	6.9	2.00	–	–	0.062	34	53	13
Ni-3	64.7	27.1	6.8	1.40	–	–	0.041	22	64	14
Ni-4	65.3	26.1	7.4	1.19	–	–	0.036	15	70	15
RuNi-1	65.2	25.2	7.0	2.42	0.17	14	0.075	33	60	7
RuNi-2	63.6	26.2	7.1	2.90	0.19	15	0.087	38	51	11
RuNi-3	64.7	25.7	7.3	2.05	0.24	9	0.062	24	63	13
RuNi-4	65.0	26.1	6.6	2.04	0.26	8	0.062	21	66	13

Note: * Proportion of surface beneath relevant peak (%)

is slightly lower than that for Ni-2. This finding is attributable to the differences in the state of Ni^{2+} ions which exist in the water solutions of nickel nitrate differing in their pH. During impregnation at pH = 1.8, nickel occurs in the form of monomeric ions which are much smaller in size than the tetrameric nickel ions at pH = 4.8. In this context, the lower concentration of Ni on the surface of the Ni-1 catalyst can be linked with a deeper penetration of nikel ions in the course of the impregnation procedure. Hoang et al. [24] have found that during impregnation of H/ZSM-5 with Ni^{2+} at pH = 1.8 nickel can also enter the zeolite channels and exchange Brönsted protons whereas at pH = 4.8 it is deposited merely on the zeolite crystals. XPS results obtained after deconvolution show that the relative amount of Ni^0 in Ni-1 is slightly lower than in Ni-2 (by 3%), which suggests a stronger nickel-support interaction. The results of XPS also make it clear that the calcination procedure changes the Ni/Al + Si atomic ratio on the catalyst surface. Thus, the Ni-4 catalyst, which was calcined twice in air for the decomposition of nickel nitrate, shows a lower Ni/Al + Si ratio than does Ni-3, which was made subject to a single calcination in air. This suggests that during calcination in air Ni tends to migrate into the support. The migration of Ni into Al_2O_3 during calcination has been reported elsewhere [25]. As can be inferred from Table 3, the migration of Ni is concomitant with the formation of NiO species, which are strongly bound to the support and do not undergo reduction during pretreatment for XPS examinations (in H_2 flow at 500 °C for 1 h). The relative amount of Ni^0 in Ni-4 is by 7% lower than in Ni-3. It is essential to note, however, that the decrease in the Ni/Al + Si ratio may also be attributed to the growth of Ni particles.

The results of activity tests for Ni catalysts are shown in Table 4; Fig. 2. As can be seen from the data in Table 4, methyltetralins (MTs) are the main products of 1-MN conversion. The yield of the products that are completely hydrogenised, i.e. methyldekalins (MDs), was low and amounted to 3.7 wt.% at 200 °C for Ni-2. At 260 °C only traces (<0.2 wt.%) of fully hydrogenated products and traces (<0.2 wt.%) of the C_8–C_{10} fraction (alkylbenzenes) were detected. Irrespective of the method used for Ni catalyst preparation, the rise in the reaction temperature from 200 to 260 °C was parallelled by the drop in 1-MN conversion: from 88 to 95% at 200 °C to 25–30% at 260 °C. Within the entire temperature range applied, a slightly higher conversion was observed over the catalysts whose preparation involved thermal treatment in H_2 flow (Ni-1 and Ni-2) than over the catalysts calcined once (Ni-3) or twice (Ni-4) in air. Upon comparison of the conversion at 200 °C before and after the activity test cycle which included the influence of reaction temperature (Table 4),

Table 4 Effect of Ni catalyst preparation method on the activity of Ni and RuNi catalysts for 1-MN conversion (τ = 0.5 sec)

Reaction temp. (°C)	Ni catalyst	Yield (wt.%)		Conversion (%)	RuNi catalyst	Yield (wt.%)		Conversion (%)
		MDs	MTs			MDs	MTs	
200	Ni-1	1.4	92.9	94.3	RuNi-1	8.4	89.6	98.0
220		0.2	82.7	82.9		2.6	81.5	84.1
240		0.1	57.4	57.5		1.4	59.4	61.0
260		0.2	28.5	28.8		1.8	39.5	41.8
200*		0.1	91.3	91.4		1.6	93.2	94.9
200**		–	7.2	7.2		0.3	45.4	45.8
200	Ni-2	3.7	91.4	95.1	RuNi-2	15.0	83.7	98.8
220		0.6	84.6	85.2		3.6	79.3	83.0
240		0.2	60.5	60.8		1.4	60.4	62.0
260		0.2	30.7	31.0		1.5	41.2	43.1
200*		0.1	94.1	94.4		2.1	95.4	97.6
200**		–	5.9	5.9		–	56.1	56.2
200	Ni-3	1.7	89.5	91.2	RuNi-3	11.8	85.1	96.9
220		0.3	85.0	85.3		2.8	81.6	84.4
240		0.2	60.4	60.7		1.1	58.9	60.1
260		0.2	27.9	28.2		0.9	37.0	38.1
200*		0.2	82.2	82.5		3.2	92.4	95.6
200**		–	2.5	2.5		–	32.2	32.2
200	Ni-4	0.7	87.6	88.3	RuNi-4	3.7	92.0	95.7
220		0.2	79.5	79.8		1.3	80.1	81.4
240		0.1	55.9	56.1		0.6	57.2	57.8
260		0.1	24.6	24.8		0.7	35.7	36.4
200*		0.1	65.6	65.8		1.4	94.4	95.8
200**		–	2.4	2.4		–	22.1	22.1

* After activity test cycle including the effect of reaction temperature

** After the whole activity test including the effect of both temperature and contact time

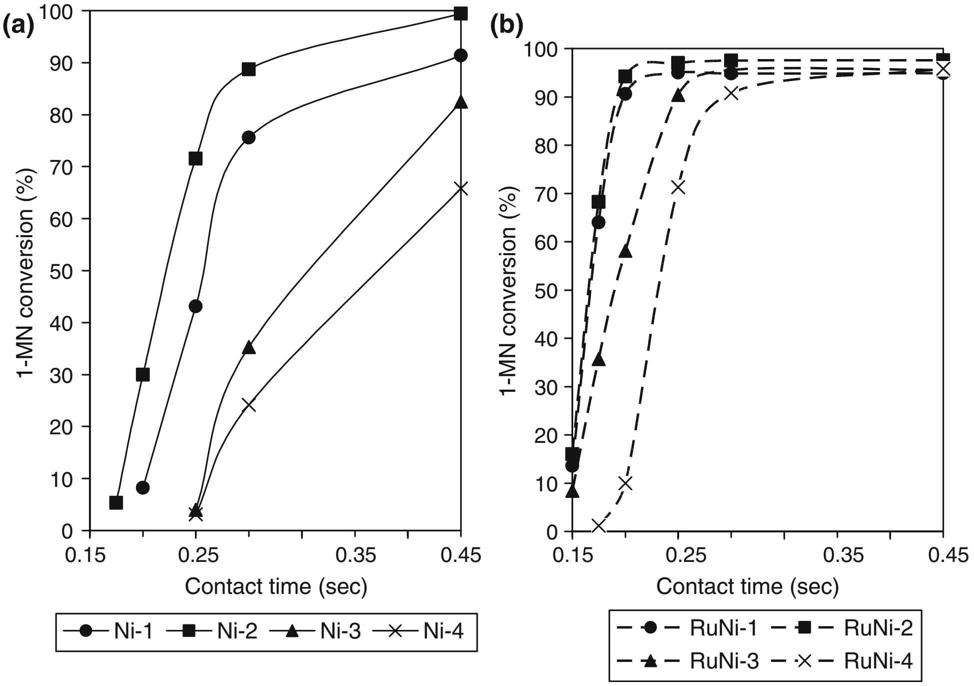

Fig. 2 Effect of contact time on 1-MN conversion over Ni (**a**) and RuNi (**b**) catalysts

the stability of the catalysts can be ordered as follows: (drop in conversion by) Ni-2 (0.7%) > Ni-1 (2.9%) > Ni-3 (8.7%) > Ni-4 (22.5%). As can be seen, Ni-4 shows the lowest activity and also the lowest stability.

The higher activity and stability of Ni-2 and Ni-1 was confirmed by activity tests involving various contact times (0.15–0.5 s) (Fig. 2a). Thus, at $\tau = 0.25$ s, Ni-4 and Ni-3 were practically inactive while over Ni-1 and Ni-2 the conversion of 1-MN amounted to 43 and 71%, respectively. It is worth noting that the decrease in catalytic activity results not only from the shortening of contact time but also from catalyst deactivation. This finding has been confirmed by the value of 1-MN conversion obtained at 200 °C ($\tau = 0.5$ s) after the whole activity test cycle (effect of temperature and contact time); the activity of the Ni catalysts was low, and the conversion of 1-MN failed to exceed 7% (Table 4).

The results of our study clearly show that the method of Ni incorporation and specifically the conditions for the thermal decomposition of nickel nitrate exert a substantial effect on the activity and stability of Ni catalysts. The catalytic properties of Ni-1 and Ni-2, whose preparation involved treatment in H_2 flow, are higher than those of Ni-3 and Ni-4, whose preparation included single or twofold calcination in air; the lowest activity was found to be that of Ni-4. Calcination in air is parallelled by an extensive migration of Ni to the support (as can be inferred from the Ni/Al + Si ratios) and by the formation of Ni oxide species that are difficult to reduce (TPR, XPS). The differences in activity between the catalysts obtained by one-step impregnation at various pH values result from the differences in the state of the Ni^{2+} ions which exist in the water solutions of nickel nitrate. During impregnation at pH = 1.8, Ni ions easier migrate to the support than at pH = 4.8, and thus enhance the nickel-support interaction in the case of Ni-1, and so the amount of such Ni oxide species that are reducible under the conditions applied prior to activity mesurements (H_2 flow, 500 °C for 1 h) is lower than in the case of Ni-2. These findings (migration of Ni and formation of Ni oxide species that are difficult to reduce) are substantiated by the measured values of H_2-chemisorption (volume of hydrogen adsorbed, metal surface available for hydrogen, and Ni dispersion). Summing up, the activity and stability of the Ni catalysts can be ordered as follows: Ni-2 > Ni-1 > Ni-3 > Ni-4, which is consistent with the decreasing reducibility of the Ni oxide species, the decreasing dispersion, and the decreasing Ni/Al + Si ratio on the catalyst surface.

3.2 RuNi Catalysts

The data in Table 2 make it clear that the textures of the RuNi catalysts are comparable to those of Ni catalysts even though the surface areas of RuNi catalysts are by 15–30 m^2/g lower as compared to those of Ni catalysts. The decrease in micropore volume suggests that the channels are occupied or blocked by Ru species. The acidity of RuNi catalysts varies from 0.89 to 0.94 mmol NH_3/g and is lower by 0.05 mmol/g as compared to Ni catalysts. It seems that Ru has covered the acid sites with metal clusters. The XRD diffractograms for the RuNi catalysts are similar (results not shown). None of the catalysts tested shows X-ray diffraction lines characteristic for Ni and Ru phase. As for the volume of the H_2 adsorbed, the catalysts can be ordered as follows: RuNi-4 < RuNi-3 < RuNi-1 < RuNi-2.

From the TPR patterns for all the RuNi catalysts it can be seen that the main reduction peak at 200–450 °C has either a small peak or a shoulder with a maximum at 500 °C. When the preparation of RuNi-3 and RuNi-4 involved calcination after stage F, the TPR shows additional high temperature peaks with maxima at 780 °C (similarly to relevant Ni catalysts).

The TPR patterns for RuNi-3 and RuNi-4 show small peaks with a maximum at about 150 °C, which is characteristic for RuO_2 reduction [8] and suggests that RuO_2 tends to occur as a separate phase. However, the calculated values of hydrogen uptake imply that a certain amount of Ru occurs in the form of bimetallic NiRu oxide clusters. Apparently, only the presence of such clusters can be expected in the other two catalysts (the TPR patterns do not include the characteristic peak for RuO_2 reduction). The formation of bimetallic NiRu oxide clusters is favoured by the procedure applied for the metal salt decomposition. In the case of the RuNi-1, RuNi-2 and RuNi-3 catalysts, Ru precursors were incorporated either into the $Ni(NO_3)_2$/ZSM-5 + Al_2O_3 or into the NiO/$Ni(NO_3)_2$/ZSM-5 + Al_2O_3 system; thereafter the metal precursors were simultaneously decomposed in H_2 flow, and that is why Ni and Ru are in close interaction with each other. In the case of the RuNi-4 catalyst, a slightly greater proportion of hydrogen uptake beneath the RuO_2 reduction peak is observed, since the Ru precursor was incorporated into a system that did not include $Ni(NO_3)_2$, i.e., into NiO/ZSM-5 + Al_2O_3. Reports on the formation of Ni–Ru clusters can be found in the literature [7, 8, 26].

The modification of Ni catalysts with Ru noticeably increased their reducibility. As can be seen from the TPR patterns (Fig. 1), hydrogen uptake in NiRu catalysts begins at temperatures by approximately 100 °C lower than in Ni catalysts. Regardless of the method used for Ni catalyst preparation, there is a shift of the low temperature peaks for Ni catalysts by 50–70 °C. This shift is linked with the formation of shoulders at 500 °C and with a decrease in the amount of the NiO species that are most difficult to reduce.

The XPS results have revealed that the relative concentration of nickel atoms is higher on the surface of the RuNi catalyst than on the surfaces of Ni catalysts. This implies that during treatment in the stream of H_2 Ni atoms migrate to the catalyst surface. This finding has also been reported by Rynkowski et al. [27] (who investigated Ni–Pt systems) and by Crisafulli et al. (who examined Ru–Cu systems [28] and Ru–Ni systems [7]). According to Crisafulli [7], the Ru precursor (which reduces at a lower temperature than Ni does) forms a nucleation centre. On top of this centre, Ni atoms (having a lower sublimation heat as compared to Ru) are deposited when Ni reduction initiates. It seems worth noting that the XPS results, similarly to those of the TPR, indicate that upon Ru incorporation the reducibility of the nickel species increases. In the case of RuNi-1, the highest decrease is observed in the relative amount of NiAl spinels that are difficult to reduce. As for the other RuNi catalysts, the decrease is parallelled by an increase in the relative amount of Ni^0 (by 2–6%).

As was expected, the modification of the Ni catalyst with Ru enhanced the activity of the catalysts. Activity results show that the effect of Ru is particularly distinct for Ni-4; at 200 °C, conversion increased by 8% (Table 4). At 260 °C, the conversion of 1-MN over all the RuNi catalysts tested is by 10–13% higher as compared to Ni catalysts. Analysis of product distribution has revealed that the incorporation of Ru enhanced catalyst selectivity towards the hydrogenation of the second ring of 1-MN. The highest yield of MDs (15.0 wt.%) was observed over RuNi-2 at 200 °C. At 260 °C, the yield of MDs and the yield of the C_8–C_{10} fraction over all the catalysts examined did not exceed 2.0 and 0.5 wt.%, respectively. The modifying effect of Ru manifests particularly in the test cycle involving variations in contact time (Fig. 1b). At the contact time of $\tau = 0.3$ and 0.5 s, the conversions over all Ni–Ru catalysts exceed 90 wt.% and are comparable. The differences in the catalyst activities are more distinct at shorter contact time, specifically at that below 0.25 s. At $\tau = 0.2$, RuNi-1 and RuNi-2 are still active, however, over RuNi-3 and RuNi-4, the conversion decreased to 58% and 10%, respectively. RuNi catalysts are more stable than Ni catalysts. Activities measured at 200 °C before and after the test cycle which involved the temperature range of 200 to 260 °C (Table 4) have revealed only a slightly decrease in 1-MN conversion. The activity values obtained at 200 °C after the whole activity test clearly substantiate the higher stability of the Ni-Ru catalysts; the highest 1-MN conversions were those over RuNi-1 and RuNi-2, amounting to 46% and 56 wt.%, respectively.

The modification of the Ni catalysts with Ru also reduced the differences in the activity of the RuNi catalysts that resulted from the various methods used for Ni incorporation, as well as from the calcination procedure applied. The enhancement in activity and reduction in activity-related differences are associated with the presence of Ru which is characterised by a high hydrogenating activity, with the occurrence of a certain amount of Ru in the form of easily reducible bimetallic NiRu oxide clusters, and (last not least) with the fact that Ru increases the reducibility of Ni oxide species (TPR). Seemingly, the favoured NiO reduction can be attributed to the fact that RuO_2 is reduced first, and thus activates hydrogen and evokes the spillover effect [6]. The higher activity of RuNi catalysts than that of the Ni catalyst is also associated with the increased concentration of nickel atoms on the surface of the RuNi catalyst than on the surfaces of Ni catalysts.

The most substantial changes attributable to Ru incorporation are observed in the less active catalysts. Our results indicate that this is due to the greater increase in their reducibility (hydrogen uptake up to 500 °C, Table 2), shown by the comparison of Ni-3 with RuNi-3 and Ni-4 with RuNi-4, which amounted to 28% and 45%, respectively. The rise in reducibility illustrated by the comparison of Ni-1 with RuNi-1 and Ni-2 with RuNi-2 approached 15% and 19%, respectively. Similar conclusions can be drawn from the comparison of the Ni surface exposure (Table 3). The atomic Ni/Al + Si ratio for RuNi-4 and RuNi-3 is higher by 72% and 51%, respectively as compared to the relevant Ni catalyst. However, for RuNi-2 and RuNi-1 the ratio is by 40% higher (as compared to relevant Ni catalyst).

Considering the stability of the catalysts (comparison of conversion before and after the activity test cycle), which is higher for RuNi than Ni catalysts, it can tentatively be assumed that the hydrogenation of the coke precursors adsorbed is favoured in the presence of the catalysts which include not only Ru as a second metal [9, 10] but also a larger quantity of Ni atoms on their surfaces. In this context it is also possible to explain why the stability of RuNi-2 is higher than the stability of the other Ru-modified catalysts (the highest Ni/Al + Si ratio).

4 Conclusions

The physicochemical properties of Ni and RuNi catalysts supported on ZSM-5 + Al_2O_3 and their catalytic performance for 1-MN hydrogenation have been studied, which enabled the following conclusions to be drawn: (i) the use of calcination in air for the decomposition of nickel nitrate deteriorates the activity and stability of the Ni catalyst to the greatest extent. Calcination is parallelled by an extensive migration of Ni to the support and the formation of Ni oxide species that are difficult to reduce; (ii) the Ni catalyst obtained by impregnation using the solution of nickel nitrate at pH = 1.8 is less active than the one obtained at pH = 4.8, because of the easier migration of Ni ions into the support; (iii) Ru not only enhances the activity and stability of the Ni catalysts but also reduces the differences in their activity resulting from the various preparation methods used. The most substantial changes induced by Ru incorporation are observed in the least active catalysts; (iv) the higher concentration of nickel atoms observed on the surfaces of the RuNi catalysts than on the surfaces of the relevant Ni catalysts also seems to have contributed to the increase in stability.

Acknowledgement Financial support by the Ministry of Science and Higher Education is gratefully acknowledged (N205 066 31/3012).

References

1. Cooper BH, Donnis BBL (1996) Appl Catal A: Gen 137:203
2. Skręt I (2000) Bull Inst Pet Process XII/4:296. ISSN 1233–3867
3. Masalska A (2008) Catal Today 137:439
4. Kotanigawa T, Yamamoto M, Yoshida T (1997) Appl Catal A: Gen 164:323
5. Arcoya A, Seoane XL, Gómez-Sainero LM (2003) Appl Surf Sci 211:341
6. Eliche-Quesada D, Mérida-Robles JM, Rodríguez-Castellón E, Jiménez-López A (2005) Appl Catal A: Gen 279:209
7. Crisafulli C, Scire S, Minico S, Solarino L (2002) Appl Catal A: Gen 225:1
8. Rynkowski JM, Paryjczak T, Lennik M (1995) Appl Catal A: Gen 126:257
9. Barrio VL, Arias PL, Cambra JF, Güemez MB, Pawelec B, Fierro JLG (2003) Appl Catal A: Gen 242:17
10. Ishihara A, Qian EW, Finahari IN, Sutrisna IP, Kabe T (2005) Fuel 84:1462
11. Cordoba G, Fierro JLG, Lopez-Gaona A, Martin N, Viniegra M (1995) J Mol Catal A: Chem 96:155
12. Li Ch, Chen YW (1995) Thermochim Acta 256:457
13. Richardson JT, Twigg MV (1998) Appl Catal A: Gen 167:57
14. Gil A, Diaz A, Gandia LM, Montes M (1994) Appl Catal A: Gen 109:167
15. Salagre P, Fierro JLG, Medina F, Sueiras JE (1996) J Mol Catal A: Chem 106:125
16. Tian P, Blanchard J, Fajerwerg K, Breysse M, Vrinat M, Liu Z (2003) Microporous Mesoporous Mater 60:197
17. Mazzieri V, Coloma-Pascual F, Arcoya A, L'Argentiére PC, Fígoli NS (2003) Appl Surf Sci 210:222
18. Masalska A (2005) Appl Catal A: Gen 294:260
19. Pawelec B, Mariscal R, Navarro RM, Campos-Martin JM, Ferro JLG (2004) Appl Catal A: Gen 262:155
20. Long-Xiang T, Feng-Mei Z, Lu-bin Z (1996) React Kinet Catal Lett 57:99
21. Rynkowski JM, Paryjczak T, Lennik M (1993) Appl Catal A: Gen 106:73
22. Petti TF, Tomczak D, Pereira CJ, Ch W, Cheng (1998) Appl Catal A: Gen 169:95
23. Kharat AN, Pendleton P, Badalyan A, Abedini M, Amini MM (2002) J Catal 205:7
24. Hoang DL, Berndt H, Miessner H, Schreier E, Völter J, Lieske H (1994) Appl Catal A: Gen 114:295
25. Kriz JF, Shimada H, Yoshimura Y, Matsubayashi N, Nishijima A (1995) Fuel 74:1852
26. Crisafulli C, Scire S, Maggiore R, Minico S, Galvagno S (1999) Catal Lett 59:21
27. Rynkowski JM, Paryjczak T, Lennik M, Farbotko M, Góralski J (1995) J Chem Soc, Faraday Trans 91:3481
28. Crisafulli C, Maggiore R, Scire S, Galvagno S (1994) J Chem Soc, Faraday Trans 90:2809